J|A|C|S
ARTICLES
Published on Web 04/17/2004

Inhibitors of ADP-Ribosylating Bacterial Toxins Based on Oxacarbenium Ion Character at Their Transition States

Guo-Chun Zhou,[†] Sapan L. Parikh,[†] Peter C. Tyler,[‡] Gary B. Evans,[‡] Richard H. Furneaux,[‡] Olga V. Zubkova,[‡] Paul A. Benjes,[‡] and Vern L. Schramm*,[†]

Contribution from the Department of Biochemistry, Albert Einstein College of Medicine, Bronx, New York 10461, and Carbohydrate Chemistry Team, Industrial Research Ltd., Lower Hutt, New Zealand

Received August 27, 2003; E-mail: vern@aecom.yu.edu

Abstract: The bacterial exotoxins, cholera toxin (CT), pertussis toxin (PT), and diphtheria toxin (DT), interfere with specific host proteins to cause tissue damage for their respective infections. The common toxic mechanism for these agents is mono-ADP-ribosylation of specific amino acids in $G_{s\alpha}$, $G_{i\alpha}$, and eEF-2 proteins, respectively, by the catalytic A chains of the toxins (CTA, PTA, and DTA). In the absence of acceptor proteins, these toxins also act as NAD^+-N-ribosyl hydrolases. The transition-state structures for NAD^+ hydrolysis and ADP-ribosylation reactions have oxacarbenium ion character in the ribose. We designed and synthesized analogues of NAD^+ to resemble their oxacarbenium ion transition states. Inhibitors with oxacarbenium mimics replacing the NMN-ribosyl group of NAD^+ show 200−620-fold increased affinity in the hydrolytic and *N*-ribosyl transferase reactions catalyzed by CTA. These analogues are also inhibitors for the hydrolysis of NAD^+ by PTA with K_i values of 24−40 μM, but bind with similar affinity to the NAD^+ substrates. Inhibition of the NAD^+ hydrolysis and ADP-ribosyl transferase reactions of DTA gave K_i values from 19 to 48 μM. Catalytic rate enhancements by the bacterial exotoxins are small, and thus transition-state analogues cannot capture large energies of activation. In the cases of DTA and PTA, analogues known to resemble the transition states bind with approximately the same affinity as substrates. Transition-state analogue interrogation of the bacterial toxins indicates that CTA gains catalytic efficiency from modest transition-state stabilization, but DTA and PTA catalyze ADP-ribosyl transferase reactions more from ground-state destabilization. pH dependence of inhibitor action indicated that both neutral and cationic forms of transition-state analogues bind to DTA with similar affinity. The origin of this similarity is proposed to reside in the cationic nature of NAD^+ both as substrate and at the transition state.

Introduction

Cholera toxin (CT), pertussis toxin (PT), and diphtheria toxin (DT) are exotoxins produced by *Vibro cholerae*, *Bordatella pertussis*, and *Corynebacterium diphtheriae* and are the causative agents of the severe diarrhea and dehydration in cholera, the whooping cough of pertussis, and the mucous membrane damage in diphtheria. Decreases in childhood immunization and world health programs make it of interest to develop new antitoxin technologies. Targeting exotoxins with specific inhibitors is an advantage over cytotoxic antibiotics since bacterial resistance is not expected to develop with antitoxins.

CT is a hetero-oligomeric toxin composed of a binding pentamer of B subunits and a loosely associated catalytic A subunit (27.2 kDa), which enters the cytosol to exert CT's toxicity.[1] Reduction of the disulfide bonds in the A subunit yields the catalytically active A1 polypeptide (CTA) (21.8 kDa) and nonactive A2 polypeptide (5.4 kDa).[2] PT is also a hexameric protein with a molecular mass of 105 kDa and has an A−B subunit structure.[3] The catalytically active subunit is the 28 kDa A protomer (PTA), which is activated by reduction of its internal disulfide bond.[4] The B protomer consists of five subunits and is responsible for receptor recognition and passage of the A protomer through the cell membrane and into the cytosol. DT is a single-chain, 535-residue (60 kDa) proenzyme. After selective proteolysis and reduction, two fragments, A and B (21 kDa and 39 kDa, respectively), are formed.[5] Fragment A (DTA) is the catalytic peptide.[6]

These bacterial exotoxins have a common mechanism in the use of NAD^+ as an ADP-ribose donor to ADP-ribosylate specific host proteins (Figure 1).[7] CTA ADP-ribosylates the

[†] Albert Einstein College of Medicine.
[‡] Industrial Research Ltd.

(1) (a) Zhang, R.-G.; Westbrook, M. L.; Westbrook, E. M.; Scott, D. L.; Otwinowski, Z.; Maulik, P. R.; Reed, R. A.; Shipley, G. G. *J. Mol. Biol.* **1995**, *251*, 550−562. (b) Zhang, R.-G.; Scott, D. L.; Westbrook, M. L.; Nance, S.; Spangler, B. D.; Shipley, G. G.; Westbrook, E. M. *J. Mol. Biol.* **1995**, *251*, 563−573.
(2) Mekalanos, J. J.; Collier, R. J.; Romig, W. R. *J. Biol. Chem.* **1979**, *254*, 5855−5861.
(3) Tamura, M.; Nagimori, K.; Murai, S.; Yajima, M.; Ito, K.; Katada, T.; Ui, M.; Ishii, S. *Biochemistry* **1982**, *21*, 5516−5522.
(4) (a) Moss, J.; Stanley, S. J.; Burns, D. L.; Hsia, J. A.; Yost, D. A.; Myers, G. A.; Hewlett, E. L. *J. Biol. Chem.* **1983**, *258*, 11879−11882. (b) Locht, C.; Antoine, R. *Biochimie* **1995**, *77*, 333−340.
(5) Lory, S.; Collier, R. J. *Proc. Natl. Acad. Sci. U.S.A.* **1980**, *77*, 267−271.
(6) Lory, S.; Carroll, S. F.; Bernard, P. D.; Collier, R. J. *J. Biol. Chem.* **1980**, *255*, 12011−12015.
(7) Van Ness, B. G.; Howard, J. B.; Bodley, J. W. *J. Biol. Chem.* **1980**, *255*, 10710−10716.

10.1021/ja038159+ CCC: $27.50

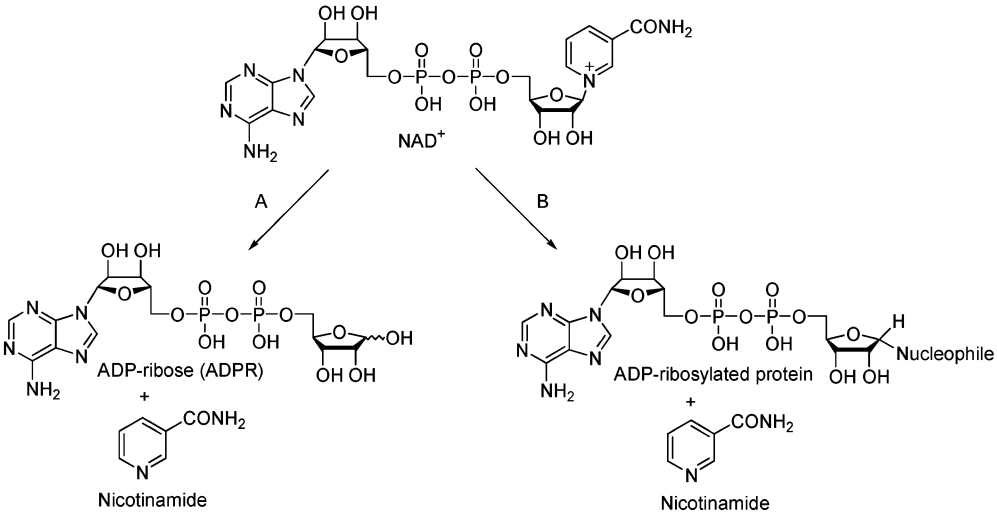

Figure 1. Route "A" is NAD^+ hydrolysis, and route "B" is ADP-ribosylation by bacterial exotoxins. The nucleophile in the CTA reaction is Arg 201 in $G_{s\alpha}$. In PTA, the nucleophile is the thiolate anion of a Cys four amino acids from the C terminal residue in $G_{i\alpha}$. In DTA the nucleophile is the imidazole nitrogen of diphthamide, a modified histidine in eEF-2 (see details in the text).

α-subunit of stimulatory GTP binding protein $G_{s\alpha}$ at Arg201[8−10] with the inversion of stereochemical configuration in the *N*-ribosidic bond. $G_{s\alpha}$ is a dual-function protein that stimulates adenylate cyclase after it binds GTP. The slow hydrolysis of its bound GTP through its intrinsic GTPase activity[11−13] returns $G_{s\alpha}$ to its resting state. ADP-ribosylation of $G_{s\alpha}$ results in the inhibition of $G_{s\alpha}$'s intrinsic GTPase activity,[14] leading to continuous stimulation of adenylate cyclase to result in high concentration of intracellular cAMP. This perturbation of the signaling pathway causes the net efflux of ions and water into the lumen of the small intestine.[15] PTA ADP-ribosylates the α-subunit of inhibitory GTP binding protein $G_{i\alpha}$ at the cysteine residue, four amino acids from the carboxyl terminus,[16] also with inversion of configuration at the thio-ribosyl bond. $G_{i\alpha}$ functions to inhibit adenylate cyclase when activated by GTP binding and also exbihits the intrinsic GTPase activity.[14] ADP-ribosylation of $G_{i\alpha}$ reduces GTPase activity of $G_{i\alpha}$ and causes continuous inhibition of the adenylate cyclase, resulting in lower blood glucose and hypersensitivity to histamine.[4b] DTA catalyzes ADP-ribosylation of a post-translationally modified histidine (diphthamide) on eukaryotic elongation factor 2 (eEF-2) and this reaction also demonstrates inversion of ribosyl stereochemistry from β to α for the *N*-ribosidic bond. ADP-ribosylated EF-2 is inactive in mediating polypeptide chain elongation in ribosomal function and results in cell death.[17] In the absence of their physiological target proteins, these toxins act as NAD^+ glycohydrolases to slowly hydrolyze NAD^+ to ADP-ribose and nicotinamide (Figure 1).[18]

The family of ADP-ribosylating exotoxins is the main cause of human tissue damage from their respective bacterial infections. Therefore, they are targets for development of new site-specific treatment of infectious diseases, including cholera, pertussis, diphthera and other bacterial infections that act by ADP-ribosylation exotoxins. Antitoxins are known to confer resistance in this disease model since diphtheria immunizations use inactivated exotoxin as the antigen. Efficient inhibitors of ADP-ribosyl transferases could prevent tissue damage from these infections. The inhibition of bacterial exotoxins neither inhibits bacterial growth nor places selective pressure on the bacteria. Resistant strains would not be expected to develop, and inhibitors against specific exotoxins could make a permanent addition to antibiotic therapy.

Transition-state analogues are proposed to be powerful inhibitors for the enzymes by trapping energy of catalysis as binding energy.[19] One approach to transition-state analogue design is to establish the nature of the enzymatic transition state and to synthesize chemically stable analogues with similar features.[20] Transition-state structures can be solved by analysis of multiple intrinsic kinetic isotope effects using specific isotopic labels of the normal substrates. This analysis has been accomplished for the actions of CTA on NAD^+ hydrolysis,[21] PTA on NAD^+ hydrolysis,[22] ADP-ribosylation of G-protein peptide α_{i3} C_{20}[23] and recombinant $G_{i\alpha1}$ subunits,[24] and DTA on NAD^+ hydrolysis[25] and ADP-ribosylation of eEF-2.[26] The studies have

(8) Gill, D. M. *Proc. Natl. Acad. Sci. U.S.A.* **1975**, *72*, 267−271.
(9) Gill, D. M. *J. Infect. Dis.* **1976**, *133* (Suppl.), s55−s63.
(10) Moss, J.; Vaughan, M. *J. Biol. Chem.* **1977**, *252*, 2455−2457.
(11) Casey, P. J.; Gilman, A. G. *J. Biol. Chem.* **1988**, *263*, 2577−2580.
(12) Moss, J.; Vaughan, M. *Adv. Enzymol.* **1988**, *61*, 303−379.
(13) (a) Cassel, D.; Selinger, Z. *Proc. Natl. Acad. Sci. U.S.A.* **1977**, *74*, 3307−3311. (b) Cassel, D.; Eckstein, F.; Lowe, M.; Selinger, Z. *J. Biol. Chem.* **1979**, *254*, 9835−9838. (c) Freissmuth, M.; Gilman, A. G. *J. Biol. Chem.* **1989**, *264*, 21907−21914.
(14) Hepler, J. R.; Gilman, A. G. *Trends Biochem. Sci.* **1992**, *17*, 383.
(15) (a) Keller, M. T. *Pediatr. Infect. Dis.* **1986**, *5*, 5101−5105. (b) Field, M.; Rao, M. C.; Chang, E. B. *N. Engl. J. Med.* **1989**, *321*, 800−806. (c) Field, M.; Rao, M. C.; Chang, E. B. *N. Engl. J. Med.* **1989**, *321*, 879−883.
(16) (a) Katada, T.; Ui, M. *Proc. Natl. Acad. Sci. U.S.A.* **1982**, *74*, 3129−3133. (b) West, R. E.; Jr.; Moss, J.; Vaughan, M.; Liu, T.; Liu, T.-Y. *J. Biol. Chem.* **1985**, *260*, 14428−14430.
(17) Wilson, B. A.; Collier, R. J. *Curr. Top. Microbiol. Immunol.* **1992**, *175*, 27−41.
(18) (a) Katada, T.; Tamura, M.; Ui, M. *Arch. Biochem. Biophys.* **1983**, *24*, 290−298. (b) Kandel, J.; Collier, R. J.; Chung, D. W. *J. Biol. Chem.* **1974**, *249*, 2088−2097. (c) Moss, J.; Manganiello, V. C.; Vaughan, M. *Proc. Natl. Acad. Sci. U.S.A.* **1976**, *73*, 4424−4427. (d) Moss, J.; Stanley, S. J.; Lin, M. C. *J. Biol. Chem.* **1979**, *254*, 11993−11996. (e) Galloway, T. S.; Van Heyningen, S. V. *Biochem. J.* **1987**, *244*, 225−230.
(19) Wolfenden, R. *Acc. Chem. Res.* **1972**, *5*, 10−18.
(20) Schramm, V. L. *Acc. Chem. Res.* **2003**, *36*, 588−596.
(21) Berti, P. J.; Schramm, V. L. *J. Am. Chem. Soc.* **1997**, *119*, 12069−12078.
(22) Schreuring, J.; Schramm, V. L. *Biochemistry* **1997**, *36*, 4526−4534.
(23) Schreuring, J.; Schramm, V. L. *Biochemistry* **1997**, *36*, 8215−8223.
(24) Schreuring, J.; Berti, P. J.; Schramm, V. L. *Biochemistry* **1998**, *37*, 2748−2758.
(25) Berti, P. J.; Blanke, S. R.; Schramm, V. L. *J. Am. Chem. Soc.* **1997**, *119*, 12079−12088.
(26) Parikh, S. L.; Schramm, V. L. *Biochemistry* **2004**, *43*, 1204−1212.

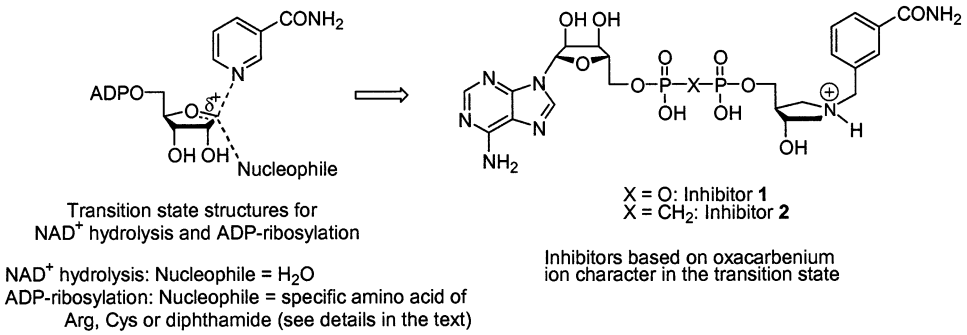

Figure 2. Transition-state structures for ADP-ribosylating toxins and features common to inhibitors **1** and **2**.

established that transition states for the ADP-ribosylation reaction all have oxacarbenium ion character in the ribose with varying degrees of nucleophilic participation by the attacking nucleophpile (Figure 2).[21−26] On the basis of these data, inhibitors **1** and **2** were synthesized to be ribooxacarbenium ion mimics of NAD^+ analogues (Figure 2). These proposed analogues of the exotoxin transition states are characterized in this report.

Experimental Section

Synthetic Procedures. *N-tert*-Butoxycarbonyl-(3*R*,4*R*)-3-acetoxy-4-acetoxymethylpyrrolidine (5). Acetic anhydride (4.5 mL, 47 mmol) was added dropwise to a stirred solution of *N-tert*-butoxycarbonyl-(3*R*,4*R*)-3-hydroxy-4-hydroxymethylpyrrolidine (**4**) (2.0 g, 9.2 mmol) in dry pyridine (15 mL) at 0 °C (Scheme 1). After 1 h at 0 °C, the resulting solution was allowed to warm to room temperature overnight, diluted with ethyl acetate (250 mL), washed with water (100 mL), dried ($MgSO_4$), and concentrated in vacuo to afford a syrup. Chromatography (ethyl acetate/petroleum ether, 1:1) gave **5** (2.5 g, 90%) as a clear syrup (Scheme 1). ^{1}H NMR ($CDCl_3$): δ 4.10 (m, 1H), 4.04 (d, J = 6.9 Hz, 2H), 3.72 (dd, J = 5.3 Hz, 1H), 3.59 (m, 1H), 3.42−3.31 (m, 2H), 2.64−2.55 (m, 1H), 2.06 (s, 6H), 1.46 (s, 9H). ^{13}C NMR: δ 171.1 (C), 170.8 (C), 170.4 (C),154.4 (C), 79.9 (CH), (74.7, 74.0) (CH), 63.3 (CH_2), 60.4 (CH), (50.8, 50.5) (CH_2), (46.9, 46.7) (CH_2), (42.6, 41.1) (CH), 28.6 (CH_3), 21.1 (CH_3), 20.9 (CH_3).

(3*R*,4*R*)-3-Acetoxy-4-acetoxymethylpyrrolidine Hydrochloride (6). A solution of hydrogen chloride in 1,4-dioxane (26 mL of 4.0 M solution) was added to a solution of **5** (2.2 g, 7.3 mmol) in dichloromethane (40 mL), and the resulting mixture was stirred for 2 h at room temperature. On completion, the reaction was concentrated in vacuo to afford **6** as the hydrochloride salt (1.7 g, 98%). ^{1}H NMR ($CDCl_3$): δ 5.13 (m, 1H), 4.13 (m, 2H), 3.69 (m, 1H), 3.62 (m, 1H), 3.40−3.27 (m, 2H), 2.75 (m, 1H), 2.04 (s, 6H). ^{13}C NMR: δ 169.9 (C),169.3 (C), 72.8 (CH), 61.2 (CH_2), 48.5 (CH_2), 45.1 (CH_2), 42.1 (CH), 20.0 (CH_3), 19.9 (CH_3).

3-Carboxamidobenzaldehyde (7). 3-Cyanobenzaldehyde (3.1 g, 23.6 mmol) in concentrated sulfuric acid (30 mL) was heated for 2 h at 100 °C. After being cooled to room temperature, the reaction mixture was diluted with ice-cold water (200 mL), extracted with ethyl acetate (3 × 100 mL), washed with saturated $NaHCO_3$, dried ($MgSO_4$), and concentrated in vacuo to afford a white solid. Recrystallization from ethyl acetae afforded **7** as a white solid (3.2 g, 91%). ^{1}H NMR (CD_3OD): δ 10.0 (s, 1H), 8.40 (s, 1H), 8.17 (d, J = 1.4 Hz, 1H), 8.08 (d, J = 1.3 Hz, 1H), 7.69 (br s, 1H), 7.66 (t, J = 1.3 Hz, 1H), 7.44 (br s, 1H).

(3*R*,4*R*)-3-[(3-Acetoxy-4-acetoxymethylpyrrolidin-1-yl)methyl]-benzamide (8). Sodium triacetoxyborohydride (2.2 g, 10.3 mmol) was added to a stirred solution of **7** (1.7 g, 11.4 mmol) and **6**•HCl (1.7 g, 7.2 mmol) in 1,2-dichloroethane (40 mL) and stirred overnight at room temperature under argon atmosphere. The reaction mixture was then washed with saturated $NaHCO_3$, dried ($MgSO_4$), and concentrated in vacuo to give a syrupy compound. Chromatography (chloroform/ethyl acetate/methanol, 5:2:1) of the resulting residue afforded **8** (2.16 g, 77%) as a syrup that was used in the next step without further purification.

(3*R*,4*R*)-3-[(3-Hydroxy-4-hydroxymethylpyrrolidin-1-yl)methyl]-benzamide (9). A solution of **8** (2.1 g, mmol) in 7 N NH_3 in methanol (30 mL) was stirred overnight at room temperature and then concentrated to dryness. Chromatography (chloroform/ethyl acetate/methanol, 5:2:1 → dichloromethane/methanol/ammonia, 7:2.5:0.5) gave **9** as a clear syrup (0.9 g, 56%). ^{1}H NMR (CD_3OD): δ 7.86 (s, 1H), 7.78 (d, J = 1.3 Hz, 1H), 7.52 (d, J = 2.6 Hz, 1H), 7.41 (t, 1H), 4.04−4.00 (m, 1H), 3.51−3.75 (m, 4H), 2.94 (t, 1H), 2.72 (m, 1H), 2.58 (dd, 1H), 2.36 (m, 1H), 2.22−2.19 (m, 1H). ^{13}C NMR: δ 175.2 (C), 142.8 (C), 138.0 (C), 136.5 (CH), 132.5 (CH), 132.2 (CH), 130.5 (CH), 77.0 (CH), 67.0, 65.9, 63.9, 60.2 (CH_2), 54.1 (CH). M/Z calculated for $C_{13}H_{19}N_2O_3$ (MH^+): 251.1396. Found: 251.1381.

(3*R*,4*R*)-3-[(3-Hydroxy-4-methanesulfonylmethylpyrrolidin-1-yl)-methyl]benzamide (10). Methanesulfonyl chloride (165 mg, 1.44 mmol) was added dropwise to a solution of **9** (300 mg, 1.2 mmol) in pyridine (2 mL) at −30 °C under argon atmosphere and stirred for 1 h. Acetic anhydride (0.3 mL, 3.1 mmol) was added to the reaction mixture at −15 °C and stirring was continued for 1 h to afford a chloroform-soluble acetate of **10**. The reaction mixture was diluted with ice-cold water (20 mL), extracted with chloroform (50 mL), washed with saturated $NaHCO_3$, dried ($MgSO_4$), and concentrated in vacuo to afford a syrup. The crude residue was deacetylated in 7 N NH_3 in methanol (10 mL) by being stirred overnight at room temperature and then concentrated to dryness. Chromatography (chloroform/ethyl acetate/methanol, 5:2:1 → 5:2:3 → chloroform/ethyl acetate/methanol/aq ammonia, 5:2:3:0.1) of the resulting residue afforded **10** (257 mg, 65%) as a clear syrup. ^{1}H NMR (CD_3OD): δ 7.89 (s, 1H), 7.81 (d, J = 1.2 Hz, 1H), 7.54 (d, J = 5.6 Hz, 1H), 7.43 (t, 1H), 4.26 (m, 2H), 4.13−4.11 (m, 1H), 3.84−3.7 (m, 2H), 3.08 (s, 3H), 3.03 (m, 1H), 2.89 (m, 1H), 2.70 (dd, 1H), 2.52−2.45 (m, 2H). ^{13}C NMR: δ 172.5 (C), 139.4 (C), 135.6 (C), 134.2 (CH), 130.1 (CH), 129.9 (CH), 128.4 (CH), 73.7 (CH), 71.8, 62.9, 60.9, 56.6 (CH_2), 50.0 (CH), 37.6 (CH_3). M/Z calcd for $C_{14}H_{21}N_2O_5S$ (MH^+): 329.1171. Found: 329.1160.

Adenosine Bisphosphonate 11. Tetrabutylammonium hydroxide (40% in water) was added to a solution of methylene diphosphonic acid (1.14 g, 6.48 mmol) in water (15 mL) until the pH was 10. The solution was lyophilized, and the residue was dissolved in acetonitrile and concentrated to dryness. A solution of this material and 2′,3′-*O*-isopropylidene-5′-*O*-toluenesulfonyladenosine (2.5 g, 5.42 mmol) in dry acetonitrile (10 mL) was stirred at room temperature for 16 h and then concentrated to dryness. The residue in water was eluted through a column of Amberlyst A15 resin (NH_4^+ form), and the eluant was concentrated to dryness. Chromatography (^{i}PrOH/H_2O/aq NH_3 8:1:1, then 6:2:2) of the residue on silica gel afforded the ammonium salt **11** (1.94 g, 69%) as a glass. ^{1}H NMR (D_2O): δ 8.33 (s, 1H), 8.08 (s, 1H), 6.12 (d, J = 3.2 Hz, 1H), 5.32 (dd, J = 3.3, 6.2 Hz, 1H), 5.14 (dd, J = 2.2, 6.2 Hz, 1H), 4.57 (s, 1H), 4.03 (m, 2H), 2.04 (dt, J = 2.5, 19.8 Hz, 2H), 1.61 (s, 3H), 1.39 (s, 3H).

Scheme 1

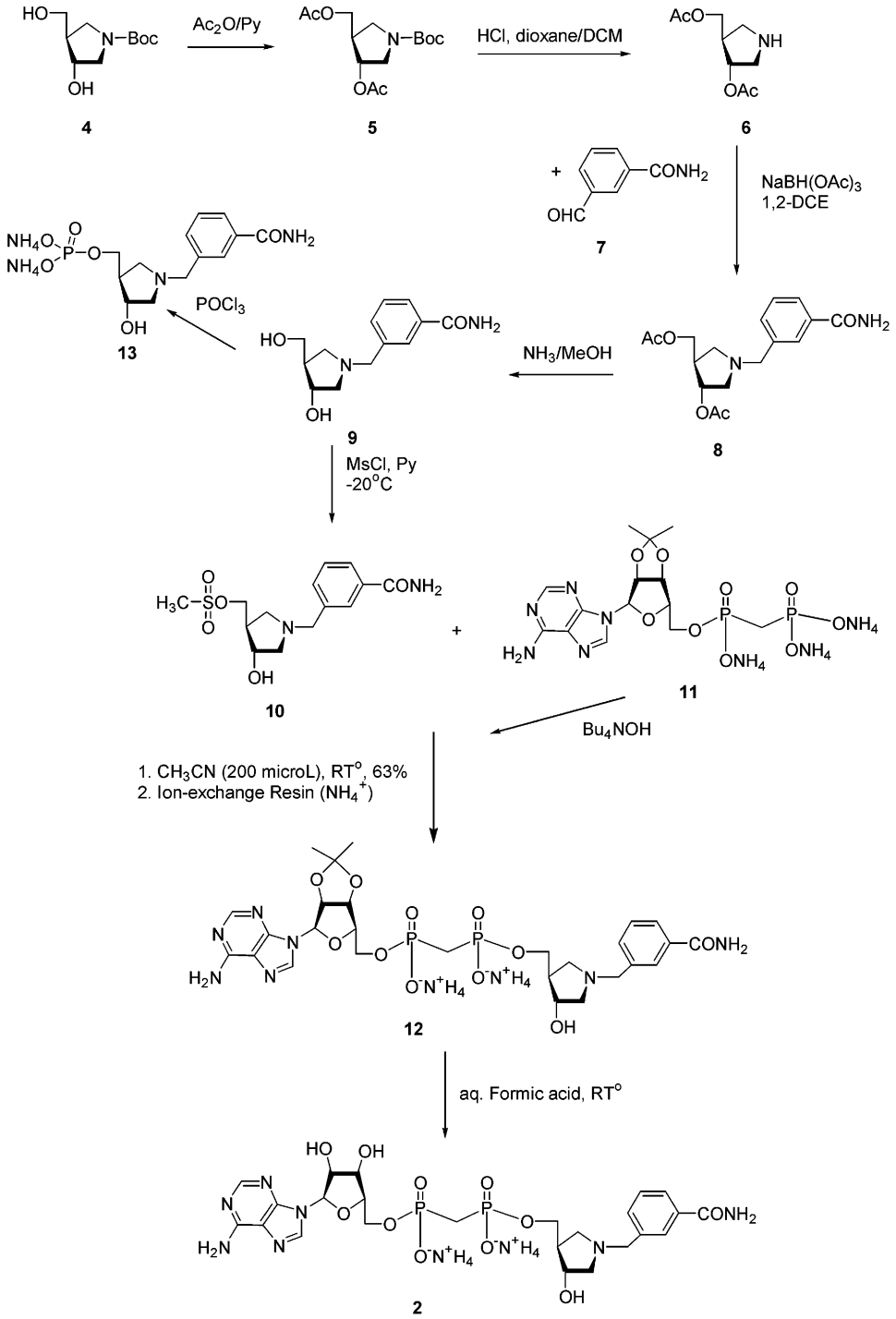

Compound 12. A solution of tetrabutylammonium hydroxide in water (40% solution, 2.13 mL, 3 equiv) was added to a solution of **11** (565 mg, 1.1 mmol) in acetonitrile (2 mL) and concentrated in vacuo to dryness. This tetrabutylammonium salt of **11** was dissolved in acetonitrile (1 mL) and added to a suspension of **10** (180 mg, 0.548 mmol) in acetonitrile (1 mL). After concentration to dryness, followed by drying in vacuo, the residue was dissolved in acetonitrile (200 μL), and the solution was stirred overnight at room temperature and then concentrated to dryness. The resulting residue was dissolved in water (2 mL) and passed through a column of Amberlyst-15, (NH_4^+ form). The crude product was purified by chromatography (^{i}PrOH/water/aq ammonia, 4:1:1) to give **12** as a white solid (240 mg, 63%), which was used in the next step without further purification. M/Z calcd for $C_{27}H_{36}N_7O_{11}P_2$ $(M - H)^-$: 696.1948. Found: 696.1952.

Compound 2. Formic acid (3 mL, 80%) was added to **12** (90 mg, 0.27 mmol) and stirred at room temperature for 5 h. The reaction mixture was diluted with water and concentrated in vacuo to dryness. Chromatography (acetonitrile/water, 4:1 → acetonitrile/water/aq ammonia, 8:1:1 → 3:1:1) afforded **2** as a white solid (56 mg, 66%). ^{1}H NMR (D_2O): δ 8.36 (s, 1H), 8.08 (s, 1H), 7.73 (s, 1H), 7.62 (d, J = 7.4 Hz, 1H), 7.55 (d, J = 7.5 Hz, 1H), 7.35 (t, 1H), 5.96 (d, J = 5.3 Hz, 1H), 4.65 (m, 1H), 4.48 (m, 1H), 4.43−4.40 (m, 2H), 4.24 (m, 2H), 3.99−3.87 (m, 4H), 3.64−3.52 (m, 2H), 2.55 (m, 2H), 2.16−2.09 (m, 2H). ^{13}C NMR: δ 171.8 (C), 154.9 (C), 152.1 (CH), 149.0

Scheme 2

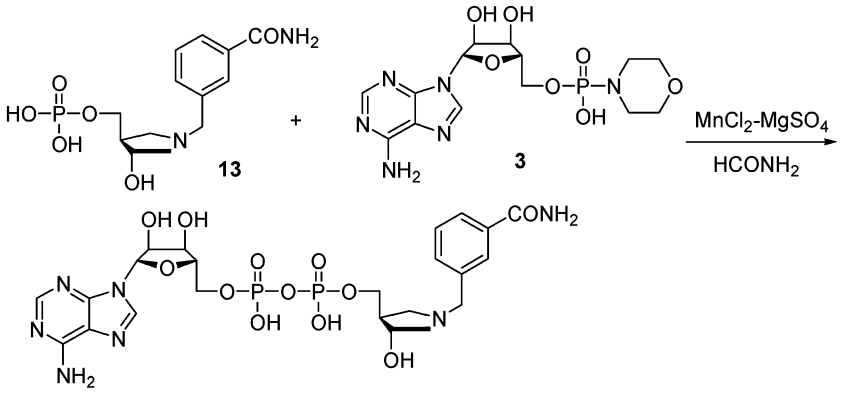

(C), 140.4 (CH), 134.5 (CH), 133.5, 130.8 (C), 129.8, 129.6, 128.9 (CH), 118.7 (C), 87.4, 84.1, 74.2, 72.3, 70.5 (CH), 64.2, 62.8, 60.4, 54.9, 49.3 (CH_2), 46.6 (CH), (28.4, 26.7, 25.0) (CH_2). M/Z calcd for $C_{24}H_{32}N_7O_{11}P_2$ $(M - H)^-$: 656.1635. Found: 656.1630.

Phosphate 13. A solution of **9** (0.06 g, 0.24 mmol) in trimethyl phosphate (2 mL) was cooled to 0 °C, and phosphoryl chloride (0.088 mL, 0.96 mmol) was added. The solution was stirred at 0 °C for 4 h and then quenched with water. Excess aq NH_3 was added, and the solution was concentrated to dryness. Chromatography afforded **13** (6 mg) as a white solid. ^{1}H NMR (D_2O): δ 7.89 (m, 2H), 7.72 (d, J = 7.8 Hz, 1H), 7.60 (t, J = 7.6 Hz, 1H), 4.53−4.48 (m, 3H), 3.95−3.82 (m, 2H), 3.78−3.69 (m, 1H), 3.63−3.58 (m, 1H), 3.38−3.29 (m, 2H), 2.61 (s, 1H).

High-resolution mass spectra were recorded on MARINER 5158 electrospray TOF mass spectrometer.

Synthesis of Inhibitor 1. Coupling of **13** and **3** was modified from literature procedures.[27−29] Briefly, 0.6 mg (1.65 μmol) of **13** as the bis-(ammonium) salt and 3.0 mg (4.2 μmol) of adenosine 5′-monophosphomorpholidate 4-morpholine-*N*,*N*′-dicyclohexylcarboxamidine salt (Sigma) were dissolved in 0.5 mL of formamide together with $MnCl_2$ (1.0 mg) and $MgSO_4$ (0.5 mg) (Scheme 2). The reaction mixture was stirred at room temperature for 2 days.

The mixture was lyophilized and reconstituted in 1 mL of water, and undissolved materials were removed by centrifugation. The aqueous extract was purified by HPLC (90% of 100 mM ammonium acetate, pH 5.0 and 10% of 50% aqueous methanol; 2 mL/min; 260 nm; 35 min). The product-containing fractions were lyophilized, and the ammonium acetate salt was removed by C18 Sep-Pak cartridge (Waters) eluted with 10 mM triethylammonium bicarbonate (TEAB) according to the procedure recommended in http://dharmacon.com. The lyophilized product yielded **1** as the bis(triethylammonium) salt (0.38 mg, 26.8%). ^{1}H NMR (D_2O): δ 1.31 (t, 18H, Et_3N), 2.15 (m, 1H), 3.10 (m, 2H), 2.23 (q, 12H, Et_3N), 3.90−4.52 (m, 10H), 6.07 (d, 1H, J = 5.85 Hz), 7.47 (m, 1H), 7.56 (m, 1H), 7.77 (m, 2H), 8.21 (s, 1H), 8.45 (s, 1H) ppm. ^{31}P NMR (D_2O): δ −9.87, −9.95 ppm. MS (ESI): 660 (M^+ + H), 761 (M^+ + H + Et_3N), 1319 ($2M^+$ + H).

General Assay Procedure. The assays are based on the enzymatic reactions of NAD^+ hydrolysis and ADP-ribosylation (Figure 1). All assays were initiated by the addition of NAD^+, including carbonyl-^{14}C radioactive labeled NAD^+. Aliquots (4 μL) were taken from the reaction mixtures at designated times and loaded onto DEAE cellulose TLC plates (EM Science) and developed in 70/30 of 95% EtOH/1 M ammonium acetate, pH 7.5.[18c] The R_f of nicotinamide is 0.9, and that of NAD^+ is 0.2. TLC plates were cut into pieces containing the NAD^+ and nicotinamide spots and quantified by liquid scintillation to determine the fraction of NAD^+ converted to nicotinamide. The inhibition of inhibitors **1** and **2** were competitive inhibitors with respect to NAD^+ (data are not shown here), and all kinetic data were fit to equations for competitive inhibition using the Kaleidagraph program (version 3.52).

Values of K_m and k_{cat} were determined by fits to the equation $v = k_{cat}\ ES/(S + K_m)$, where v is the initial rate, E is the enzyme concentration, S is the substrate (NAD^+ for $K_{m(NAD)}$ and ArgOMe for $K_{m(ArgOMe)}$) concentration, k_{cat} is the catalytic turnover number, and K_m is the Michaelis constant. The inhibition constant (K_i) values were determined by the equation $v/v_0 = (S + K_m)/(S + K_m(1 + I/K_i))$ or $v/v_1 = (S + K_m(1 + I_1/K_i))/(S + K_m(1 + I/K_i))$, where v is the initial rate with the inhibitor, v_0 is the initial rate without the inhibitor, v/v_1 is the ratio of the initial rates with two different inhibitor concentrations, S is the substrate (NAD^+) concentration, I is the inhibitor concentration, I_1 is the lowest inhibitor concentration, and K_m is the Michaelis constant.

Inhibitors **1** and **2** were tested in assays on cholera toxin A (CTA), diphtheria toxin A (DTA), and pertussis toxin A (PTA). Inhibition assays for DTA were for ADP-ribosylation of yeast eEF-2, and those for CTA were for ADP-ribosylation of ArgOMe. All toxins were tested for inhibition of NAD^+ hydrolysis.

Assays for CTA. Cholera toxin A protomer from *V. cholerae* was purchased from Sigma as a lyophilized powder containing less than 0.5% of cholera toxin B subunit according to SDS-PAGE. The A protomer was reconstituted to 1.0 mg/mL (~36.8 μM) as recommended by the supplier. The activity was assayed at 30 °C in 200 mM sodium phosphate, pH 7.5, and 20 mM DTT (dithiothreitol). The A protomer was preactivated in the buffer for 30 min at 30 °C to reduce the disulfide bond between the catalytic A_1 polypeptide (CTA) and the noncatalytic A_2 polypeptide.[2,18c]

Determination of K_m and k_{cat} of NAD^+ Hydrolysis by CTA. Reaction mixtures of 20 μL contained 3.68 μM of CTA (preactivated) and variable concentrations of NAD^+ (0.712, 2.07, 5.08, 10.1, 20.1, and 39.1 mM including 4.6, 4.0, 4.1, 3.3, 6.7, and 6.0 μCi/mL of radioactive-labeled NAD^+). Aliquots (4 μL) were taken from the reaction mixtures at 60, 120, and 180 min and applied to TLC plates.

Determination of $K_{m(NAD)}$ and k_{cat} of ADP-Ribosylation of Arginine Methyl Ester (ArgOMe) by CTA. Reaction mixtures of 20 μL contained 0.92 μM of CTA (preactivated), 75 mM ArgOMe, and variable concentrations of NAD^+ (0.994, 2.07, 2.81, 10.1, 20.1, and 37.6 mM including 4.5, 4.0, 4.5, 3.3, 6.7, and 6.3 μCi/mL of radioactive-labeled NAD^+). Aliquots (4 μL) were taken from the reaction mixtures at 90 and 120 min and applied to TLC plates.

Determination of $K_{m(ArgOMe)}$ for ADP-Ribosylation of Arginine Methyl Ester (ArgOMe) by CTA. Reaction mixtures of 20 μL contained 0.92 μM of CTA (preactivated), 2.38 mM NAD^+ containing 3.8 μCi/mL of radioactive-labeled NAD^+, and variable concentrations of ArgOMe (2.0, 10.0, 30.0, 50.0, 75.0, and 100.0 mM). Aliquots (4

(27) Schimazu, M.; Shinozuka, K.; Sawai, H. *Tetrahedron Lett*. **1990**, *31*, 235−238.
(28) Lee, J.; Churchil, H.; Choi, W.-B.; Lynch, J. E.; Roberts, F. E.; Volante, R. P.; Reider, P. J. *Chem. Commun*. **1999**, 729−730.
(29) Kennedy, K. J.; Bressi, J. C.; Gelb, M. H. *Bioorg. Med. Chem. Lett*. **2001**, *11*, 95−98.

Table 1. Kinetic Constants for NAD^+ and Inhibitors **1** and **2**

					inhibitor **1**		inhibitor **2**	
toxin	reaction	substrate	K_m (μM)	k_{cat} (min^{-1})	K_i (μM)	K_m/K_i	K_iT (μM)	K_m/K_i
CTA	NAD^+ hydrolysis	NAD^+, H_2O	10800.0	8.7	17.4	620	32.7	330
	ADP-ribosylation	NAD^+, ArgOMe	4700.0	20.0	10.9	431	23.6	200
PTA	NAD^+ hydrolysis	NAD^+, H_2O	19.2	0.66	24.4	0.78	39.7	0.48
	ADP-ribosylation	NAD^+, peptide α_{i3} C_{20}	27.0[23]	3.0[23]				
	ADP-ribosylation	NAD^+, Cys-$G_{i\alpha}$	23.0[24]	40.0[24]				
DTA	NAD^+ hydrolysis	NAD^+, H_2O	85.0[26]	0.11[26]	48.2	1.8	32.7	2.6
	ADP-ribosylation	NAD^+, diphthamide-eEF2	6.0 for NAD^+, 0.66 for eEF2[26]	182.0[26]	30.5	0.2	19.1	0.3

μL) were taken from the reaction mixtures at 30 and 60 min and applied on TLC plates.

Inhibition of CTA on NAD^+ by 1 and 2 for NAD^+ Hydrolysis. To the activated CTA (2.76 μM) were added variable concentrations of inhibitors (3.67, 14.68, 73.4, and 183.5 μM of **1** or 5, 20, 80, 150, 300, and 500 μM of **2**) and 2.07 mM of NAD^+ (3.8 μCi/mL of radioactive-labeled NAD^+) in a final volume of 20 μL. Aliquots (4 μL) were taken from the reaction mixtures at 120 and 180 min and applied to TLC plates. Initial rates for these reaction conditions were maintained for 240 min.

Inhibition of CTA by 1 and 2 for ADP-Ribosylation of ArgOMe. Initial rate assays (20 μL) included 0.92 μM of activated CTA, variable concentrations of inhibitors (3.67, 14.68, 73.4, and 183.5 μM of **1** or 5, 20, 80, 150, 300, and 500 μM of **2**), 75 mM of ArgOMe, and 2.36 mM of NAD^+ (4.0 μCi/mL of radioactive-labeled NAD^+). Aliquots (4 μL) were taken from the reaction mixtures at 90 and 120 min and applied on TLC plates. Reaction rates were linear for over 120 min.

Assays for PTA. Pertussis toxin A protomer (PTA, produced by *B. pertussis*) was purchased from List Biological Laboratories, Inc. It was reconstituted to 0.71 μM as recommended by the supplier. The assays were conducted at 37 °C in 100 mM Tris·HCl, pH 8.0, 1 mM EDTA, and 20 mM DTT. The A protomer (PTA) was preactivated in the buffer at room temperature for 30 min.[22−24]

Determination of K_m and k_{cat} for NAD^+ Hydrolysis by CTA. Reaction mixtures of 20 μL contained 0.143 μM of PTA (preactivated) and variable concentrations of NAD^+ (10.0, 20.0, 50.0, 92.6, 183.0, and 319.0 μM including 0.54, 1.08, 2.7, 5.0, 4.5, and 3.75 μCi/mL of radioactive-labeled NAD^+). Aliquots (4 μL) were taken from the reaction mixtures at 120 and 180 min and applied on TLC plates.

Hydrolysis of NAD^+ by PTA and Inhibition by 1 and 2. Assays were conducted in reaction mixtures (30 μL) of 0.143 μM activated PTA, variable concentrations of inhibitors (3.67, 14.68, 73.4, and 183.5 μM of **1** or 5, 20, 80, 150, 300, and 500 μM of **2**), and 50 μM of NAD^+ (2.7 μCi/mL of radioactive-labeled NAD^+). Aliquots (4 μL) were taken from the reaction mixtures after incubation for 3 h and applied to TLC plates.

Assays for DTA. Recombinant DTA was overexpressed and purified to homogeneity.[25] eEF-2 is the acceptor of ADP-ribosylation by DTA and was purified from *Saccharomyces cerevisiae* according to reported procedures.[30] The activity was assayed at 37 °C in 100 mM Tris·HCl, pH 8.0, 1 mM EDTA, and 20 mM DTT.

Hydrolysis of NAD^+ and Inhibition by 1 and 2. Assays were conducted in reaction mixtures (30 μL) of 6 μM of recombinant DTA, variable concentrations of inhibitors (14.68, 73.4, 183.5, and 367.0 μM of **1** or 20, 80, 150, 300, and 500 μM of **2**), and 0.33 mM of NAD^+ (4.8 μCi/mL of radioactive-labeled NAD^+). Aliquots (4 μL) were taken from the reaction mixture after being incubated for 240 min and were applied to TLC plates.

ADP-Ribosylation of eEF-2 by DTA and Inhibition by 1 and 2. Initial rate assays (30 μL) included 670 pM (for **1**) or 500 pM (for **2**) of recombinant DTA, variable concentrations of inhibitors (3.67, 14.68, 73.4, and 183.5 μM of **1** or 5, 20, 80, 150, 300, and 500 μM of **2**), 6.7 μM of eEF-2, and 15.4 μM of NAD^+ (4.8 μCi/mL of radioactive-labeled NAD^+). Aliquots (4 μL) were taken from the reaction mixtures at 6, 10, and 15 min for **1** or 4, 7, and 12 min for **2** and applied to TLC plates.

Assays for pH dependence of kinetic parameters consisted of 200 μL reaction mixtures of 100 mM Tris-HCl (pH 7.0 to 9.0), 1 mM EDTA, 20 mM DTT, and 0.8 nM of diphtheria toxin. Assays contained 200 000 cpm [^{32}P]NAD^+ to follow ADP ribosylation. The k_{cat} and K_m for eEF-2 were determined at a fixed, saturating concentration of NAD^+ (825 μM) and by varying the concentration of eEF-2 (0.5 to 25 μM). k_{cat} and K_m for NAD^+ were determined at a fixed, saturating concentration of eEF-2 (10 μM) and by varying the concentration of NAD^+ (1 to 100 μM). Aliquots (30 μL) were removed at 0, 1, 2, and 4 minutes and pipetted into 50 μL of 5 mM unlabeled NAD^+ and precipitated by adding 80 μL 30% TCA. The precipitate was washed twice with 500 μL 5% TCA solution, followed by 500 μL of acetone and dissolved in 1 mL of 10% SDS in 200 mM Tris-HCl, pH 8.0. The sample was mixed with 10 mL of scintillation fluid and analyzed by scintillation counting to quantitate radioactivity in the ADP-ribosylated product. The kinetic parameters for ADP-ribosyltransferase activity were analyzed by fitting data to the Michaelis−Menten equation from assays preformed in triplicate in at least three independent experiments. Inhibition assays included 500 pM of DTA, 10 μM eEF-2, 15 μM NAD, and variable concentration of inhibitor (5, 20, 40, 120, 240, and 480 μM of **2**). Aliquots were taken from reaction mixtures at 4, 8, and 12 min for **2** and analyzed as described above.

Results

Inhibition of CTA by 1 and 2. Hydrolysis of NAD^+ by CTA gave a K_m for NAD^+ of 10.8 ± 0.8 mM, a k_{cat} of 8.7 ± 0.3 min^{-1}, and k_{cat}/K_m = 806 M^{-1} min^{-1} (Table 1). Inhibition of this reaction by **1** and **2** gave K_i values of 17.4 ± 2.5 μM and 32.7 ± 3.3 μM (Table 1).

ADP-ribosylation of ArgOMe by CTA gave a K_m for NAD^+ of 4.7 ± 0.2 mM, a k_{cat} of 20 ± 0.3 min^{-1}, a k_{cat}/K_m = 4255 M^{-1} min^{-1}, and a K_m for ArgOMe of 114 ± 12 mM (Table 1). Inhibitors **1** and **2** gave K_i values of 10.9 ± 1.4 μM and 23.6 ± 2.0 μM (Table 1) for this reaction. Both inhibitors **1** and **2** bind to CTA with high affinity relative to NAD^+.

Inhibition of PTA by 1 and 2. The hydrolysis of NAD^+ by PTA gave a K_m value of 19.2 μM and a k_{cat} value of 0.66 min^{-1} (Table 1). Inhibition of PTA by **1** and **2** gave values for K_i of 24.4 ± 1.3 μM and 39.7 ± 2.1 μM for NAD^+ hydrolysis (Table 1). Therefore, inhibitors **1** and **2** bind to PTA with affinities similar to the substrate NAD^+.

Inhibition of DTA by 1 and 2. DTA hydrolyzes NAD^+ with kinetic constants of K_m = 85.0 ± 13.0 μM and k_{cat} = 0.11 ± 0.04 min^{-1}.[26] **1** and **2** inhibit DTA on NAD^+ hydrolysis with K_i values of 48.2 ± 1.3 μM and 32.7 ± 3.5 μM (Table 1). **1** and **2** bind slightly better than NAD^+ to DTA for the NAD^+ hydrolysis reaction.

(30) Jørgensen, R.; Carr-Schmid, A.; Ortiz, P. A.; Kinzy, T. G.; Andersen, G. R. *Acta Crystallogr.* **2002**, *D58*, 712−715.

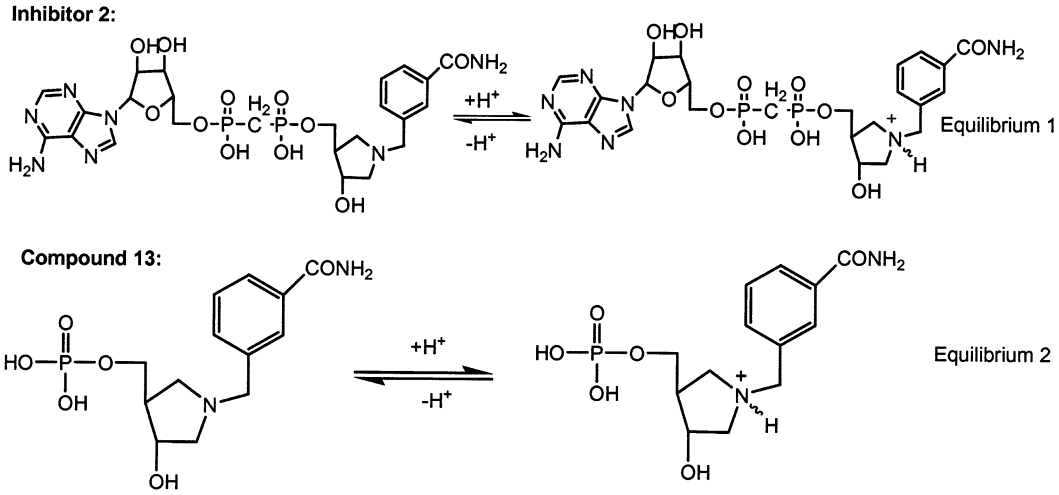

Figure 3. Ionization of inhibitors **2** and **13** to form the cationic transition-state analogues.

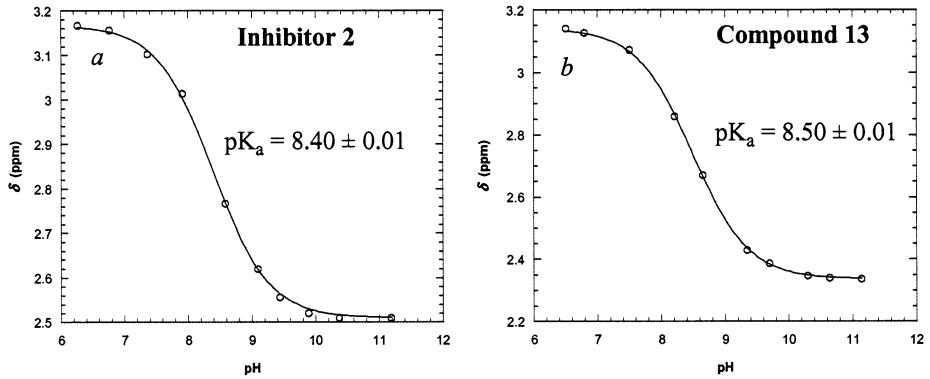

Figure 4. pK_a plots for inhibitors **2** and **13**. The chemical shift of 2′-proton resonance was followed and referenced to TSP (3-(trimethylsilyl)propionic acid) during pH titration. Titrations were in 200 mM sodium phosphate including 5% D_2O, and the data were determined from the best fit to the equation $\delta = \delta_{HA} - [(\delta_{HA} - \delta_A)/(1 + 10^{(pKa - pH)})]$,[36] where δ is the observed chemical shift value and δ_{HA} and δ_A are the chemical shift values for a given proton at the low- and high-pH limits. (a) pK_a is 8.40 for **2**. (b) pK_a is 8.50 for **13**.

DTA catalyzes the ADP-ribosylation of eEF-2 with kinetic constants of $K_{m(NAD)} = 6.0 \pm 2.0$ μM and $k_{cat} = 182 \pm 15$ min^{-1}.[26] Inhibition of DTA by **1** and **2** gave K_i values of 30.5 $\pm$ 3.3 μM and 19.1 $\pm$ 3.3 μM (Table 1) for the ADP-ribosyaltion of EF-2 by DTA. Inhibitors **1** and **2** bind to DTA less well than NAD^+ for the ADP-ribosylation of eEF-2 by DTA.

pK_a for 2 and 13 and pH Dependence of Kinetic Constants for DTA. The pK_a values for inhibitors **2** and **13** were determined by pH titration using the 2′-proton chemical shift (Figures 3 and 4). The pK_a values were readily established to be 8.40 for **2** and 8.50 for **13**. The pK_a for **1** can also be assigned as 8.40 since the chemical environment of *N*1′ is similar to that of **2**. The pH dependence for the ADP-ribosylation of eEF-2 by DTA demonstrated that the K_m values do not vary significantly from pH 7.0 to 9.0 (Table 2). Likewise, k_{cat} is independent of pH over this range. Since the primary constants are unchanged over a pH range that encompasses the pK_a of the inhibitor, altered pH can be used to test the relative inhibitory potential of the *N*1′-neutral and *N*1′-cationic inhibitors. At pH 7.0, the observed K_i is 29 μM, and the inhibitor is >90% cationic to give a calculated K_i for the cation of 27 μM, assuming the neutral form does not bind (Table 2). At pH 9.0, the K_i is 17 μM, to give a K_i of 3.4 μM if only the cation binds. Making the assumption that only *N*1′-neutral **2** binds gives calculated K_i values of 1.1 and 13.6 μM at pH 7.0 and 9.0, respectively.

Table 2. pH Dependence of DTA on NAD^+ Hydrolysis[a]

pH	7.0	7.5	8.0	8.5	9.0
K_m (μM)[b]	8.3 ± 2.0	8.5 ± 2.6	6.0 ± 2.0	5.9 ± 2.0	8.9 ± 1.7
k_{cat} (s^{-1})	3.5 ± 0.4	3.1 ± 0.3	3.0 ± 0.3	3.1 ± 0.3	3.5 ± 0.4
K_i (μM)[d]	29 ± 2	21 ± 3	19 ± 3	12 ± 2	17 ± 2
K_i (μM)[a]	27 ± 2	19 ± 3	14 ± 2	6.0 ± 0.8	3.4 ± 0.4
K_i (μM)[b]	1.1	2.3	5.4	6.7	13.6

[a] K_i for the cation of **2**, corrected by $[I]_{protonated} = p^*[I]_{total}$, where $p = 1/(1 + 10^{(ph - pK_a)})$. [b] K_i assuming only the neutral form of **2** binds to DTA.

These constants suggest that both neutral and cationic forms bind with similar dissociation constants. However, steady-state kinetic analysis cannot prove the ionic state of bound forms. Proof awaits the availability of labeled enzyme and/or inhibitor for enhanced NMR sensitivity.

Discussion

Inhibitor Design. NMR evidence has demonstrated that the reactions of ADP-ribosylation by CTA, PTA, and DTA give products characteristic of S_N2 reactions with the inversion of configuration at the 1′-anomeric carbon.[31−33] However, KIE studies and transition-state analysis demonstrate that the transition states for NAD^+ hydrolysis by CTA, PTA, and DTA are

(31) Oppenheimer, N. J. *J. Biol. Chem.* **1978**, *253*, 4907−4910.
(32) Scheuring, J.; Schramm, V. L. *J. Am. Chem. Soc.* **1995**, *117*, 12653−12654.
(33) Oppenheimer, N. J.; Bodley, J. W. *J. Biol. Chem.* **1981**, *256*, 8579−8581.

highly dissociative.[21,22,25] The transition state for ADP-ribosylation of G-protein peptide α_{i3} C_{20}[23] and recombinant $G_{i\alpha1}$ subunits[24] have more nucleophilic character at the transition state, but their transition states are also dominated by ribooxacarbenium character. Likewise, the transition state for the ADP-ribosylation of eEF-2 by DTA has increased nucleophilic participation but is dominated by its cationic character.[26] Despite their differences,[20] oxacarbenium ion character (Figure 2) is associated with all of these transition states. Inhibitors **1** and **2** were designed on the basis of the common ribooxacarbenium ion character for these transition-state structures. Recently, similar chemistry has been used to produce transition-state analogues of purine nucleoside phosphorylase and 5′-methylthioadenosine phosphorylase, *N*-ribosyltransferases with oxacarbenium character at their transition states.[34,35] In these cases, inhibitors bind 10^5 to 10^6 times tighter than substrates.

Comparison of Inhibitors. Compound **13** was tested as an exotoxin inhibitor but did not show inhibitory activity to CTA, PTA, and DTA when tested to 1000 μM (data are not shown). The ADP portion of NAD^+ is clearly important for enzyme recognition. Kinetic analysis showed that the inhibitory activity of **1** and **2** is similar for all three toxins (Table 1). Therefore, the ADP group is essential but the bridge oxygen of the pyrophosphate is not important for inhibitor recognition at any of these catalytic sites. This result is useful for the development of antitoxins, since the methylene bridge in the pyrophosphate group produces biological stability against phosphodiesterases.

Transition-State Analogue Binding to CTA. Transition-state analysis from KIE indicated that NAD^+ at the transition state of CTA is almost a fully developed ribooxacarbenium ion with bond orders of 0.02 to the nicotinamide and 0.005 to the attacking water nucleophile.[21] This expanded oxacarbenium transition state is expected to closely resemble the electrostatics of **1** and **2**. The inhibitory results demonstrate that **1** and **2** bind to CTA more strongly than NAD^+, consistent with the capture of transition-state energy.

The inhibitors **1** and **2** also have good inhibitory activity with CTA for ADP-ribosylation of ArgOMe, suggesting that the transition state of CTA on ADP-ribosylation of ArgOMe is also dissociative even though the attacking nucleophile is present at the catalytic site. However, the weak binding and poor nucleophilicity of ArgOMe is not expected to induce the same degree of nucleophilic participation as the more tightly bound $G_{s\alpha}$ nucleophiles. Nucleophilic attack lags behind transition-state formation, and the enzyme directs the stereochemistry of the reaction center (1′-C) during departure of the leaving group until the nucleophilic attack is complete. If CTA resembles DTA and PTA in its transition-state characteristics, it would be expected to be more nucleophilic in ADP-ribosyl transfer reactions than in NAD^+ hydrolysis. The nearly equivalent inhibition of CTA by **1** and **2** for hydrolytic and ArgOMe ADP-ribosyl transfer reactions supports the proposal that substantial oxacarbenium character is present at the transition state for this small-molecule acceptor of ADP-ribose.

Inhibitor Action on PTA. The K_m values for NAD^+ binding do not change much from NAD^+ hydrolysis by PTA (19.2 μM) to ADP-ribosylation of G-protein peptide α_{i3} C_{20} by PTA (27 μM)[23] and recombinant $G_{i\alpha1}$ subunits by PTA (23 μM).[24] Therefore, the interaction between NAD^+ and PTA is not strongly influenced by the nature of the nucleophile. Bond order to the water nucleophile is low at the transition state of NAD^+ hydrolysis by PTA,[22] and the major character in this transition state resides in the NAD^+ structure. The inhibitors **1** and **2** show similar binding constants (K_i = 24.4 μM for **1** and 39.7 μM for **2**) to NAD^+ (Table 1).

The catalytic rate of PTA for NAD^+ hydrolysis is k_{cat} = 0.01 s^{-1}, and this increases to 0.67 s^{-1} in the presence of saturating $G_{i\alpha}$.[24] Here, the k_{enz}/k_{chem} rate enhancement is modest for NAD^+ hydrolysis. Similar to DTA, inhibitiors **1** and **2** bind to PTA with affinity not significantly different from the Michaelis constant for NAD^+. This pattern is consistent with enzyme-based substrate destabilization, where features of the transition state will not necessarily increase binding. Catalytic evidence for substrate destabilization by CTA, DTA, and PTA is supplied by the common observation that the ADP-ribosylating toxins all catalyze the slow hydrolysis of NAD^+ in the absence of their nucleophilic ADP-ribose acceptors. Catalysis of NAD^+ hydrolysis requires that binding in the Michaelis complex destabilizes bound NAD^+ toward the transition state, facilitating the attack of the solvent water nucleophile. NAD^+ chemical destabilization is readily accomplished by the hydrophobic interactions with the nicotinamide ring discussed below.

Inhibitor Action on DTA. The transition states for the NAD^+ hydrolytic reactions of CTA and DTA are closely related, with Pauling bond orders of approximately 0.02 to the nicotinamide leaving group and 0.005 to the attacking water nucleophile.[21,22] However, their kinetic constants for K_m and k_{cat} are quite different (K_m for CTA/K_m for DTA = 125 and k_{cat} for CTA/k_{cat} for DTA = 75). Catalytic efficiency for NAD^+ hydrolysis is low for both catalysts, but the k_{cat} value of 0.15 s^{-1} for CTA greatly exceeds the rate of 0.002 s^{-1} for DTA. These slow rates place modest limits on the theoretical affinity of transition-state analogues. Wolfendens' construct for transition-state affinity assumes limits of (substrate K_d) × (k_{chem}/k_{enz}), where k_{chem} and k_{enz} are nonenzymatic and enzymatic solvolysis rates, respectively, and K_d is the dissociation constant for substrate.[19] At pH 7.5, the k_{chem} for NAD^+ under our experimental conditions is approximately 10^{-6} s^{-1}. Thus, rate enhancements are 1.5 × 10^5 for CTA but only 2 × 10^3 for DTA. The transition-state analogues capture a significant fraction of the 1.5 × 10^5 rate enhancement energy from CTA by binding up to 620-fold more tightly than NAD^+. However, in the case of DTA, where rate enhancement is only 2 × 10^3, there is insufficient recognition of the transition-state features to enhance binding. This result illustrates an inherent property of transition-state analogue design. Poor catalysts can capture only relatively small amounts of binding energy from molecules that resemble the poorly stabilized on-enzyme transition states.

The similar binding of NAD^+ and inhibitors **1** and **2** to both DTA and PTA suggest that the catalytic rate enhancement is caused by ground-state destabilization where bound NAD^+ is more reactive to solvent water in the bound than in the free state. Ground-state destabilization is easily accomplished simply by placing the nicotinamide leaving group into a hydrophobic environment. The partial positive charge on the nicotinamide group is shifted toward the ribosyl ring to make it more

(34) Lewandowicz, A.; Tyler, P. C.; Evans, G. B.; Furneaux, R. H.; Schramm, V. L. *J. Biol. Chem.* 2003, *278*, 314654−31468.
(35) Dyson, H. J.; Tennant, L. L.; Holmgren, A. *Biochemistry* **1991**, *30*, 4262−4268.

oxacarbenium-like. A hydrophobic pocket that surrounds the nicotinamide group is known to be a feature of NAD^+ binding to DTA and PTA.[24,25] The addition of eEF-2 increases the reaction rate of DTA 1600-fold, but inhibitors **1** and **2** show no improvement in affinity, also consistent with ground-state destabilization as the primary mechanism for enhancing the rate of catalysis. Inhibitors **1** and **2** do not include the contribution from the attacking nucleophile, and bindings of **1** and **2** to DTA on NAD^+ hydrolysis are only slightly better than NAD^+ binding to DTA on NAD^+ hydrolysis (Table 1).

From NAD^+ hydrolysis by DTA ($K_{m\ (NAD)} = 85\ \mu M$) to ADP-ribosylation of eEF-2 by DTA ($K_{m(NAD)} = 6.0 \pm 2.0\ \mu M$, $k_{cat} = 182 \pm 15\ min^{-1}$),[26] NAD^+ binding to DTA becomes stronger. However, the most strongly bound component of the ternary complex is eEF-2 ($K_{m(EF-2)} = 0.66 \pm 0.06\ \mu M$)[26] rather than NAD^+. The attacking nucleophile in the ADP-ribosylation of eEF-2 is diphthamide, and here the nucleophilic bond order increases from 0.005 for water (in the hydrolytic reaction) to 0.03 (in the eEF-2 reaction). The increased nucleophile participation is responsible for the 1600-fold rate acceleration relative to NAD^+ hydrolysis.

pH Profile for ADP-Ribosylation of eEF-2 by DTA. The pyrrolidine N pK_a values of **2** and **13** are 8.40 and 8.50, respectively (Figure 4). To establish the ionic form binding to DTA, the pH dependence of kinetic parameters was measured. NAD^+ is unlike other substrates for *N*-ribosyltransferases in being cationic at N1 in the substrate and being cationic at C1′ at the transition state (Figure 2). Electron migration to the leaving group nicotinamide causes the cationic center to shift from N1 of the leaving group to C1′ of the NMN-ribosyl group. Transition-state mimicry of **1** and **2** relies on the cationic nature of the transition state, but the distance of cation migration is only about 1.5 Å on conversion of substrate NAD^+ to NAD^+ at the transition state.[24,25] The K_i values measured for **2** in the ADP-ribosylation of eEF-2 by DTA show little change over 2.0 pH units, conditions where the N-cation varies from 96 to 20% of the inhibitor species. The K_m for NAD^+ also shows little pH dependence. The simplest explanation is that both neutral and cationic forms bind to the enzyme with similar K_i values of approximately 20 μM. If it is assumed that only the cationic or neutral forms bind, the K_i values would vary considerably across this pH range (Table 2). However, this kinetic argument cannot prove the ionic state of bound **2**. Direct measurement requires isotopically labeled inhibitor or enzyme or both.

Conclusions

Analogues of NAD^+ at the transition states for the ADP-ribosylating bacterial exotoxins bind more tightly to CTA, but not to DTA or PTA. CTA binds weakly to NAD^+ and gains catalytic rate enhancement from transition-state stabilization. DTA and PTA bind more tightly to NAD^+ as substrate and catalyze their respective reactions by ground-state destabilization of the NAD^+, making it more reactive to nearby nucleophiles provided by the physiological substrates, eEF-2 and $G_{i\alpha}$, as well as water nucleophiles. Since much of the catalytic rate enhancement comes from proximity of the ADP-ribosyl acceptor, transition-state analogues with only NAD^+ features bind poorly. Improved binding might be expected for analogues containing features of NAD^+ at the transition state, along with features of the nucleophilic group.

Acknowledgment. This work was supported by NIH Research Grant AI34342 and the New Zealand Foundation for Research, Science & Technology.

JA038159+